iJRASET
International Journal For Research in
Applied Science and Engineering Technology

INTERNATIONAL JOURNAL FOR RESEARCH

IN APPLIED SCIENCE & ENGINEERING TECHNOLOGY

Volume: 13 **Issue:** V **Month of publication:** May 2025

DOI: https://doi.org/10.22214/ijraset.2025.70736

International Journal for Research in Applied Science & Engineering Technology (IJRASET)
ISSN: 2321-9653; IC Value: 45.98; SJ Impact Factor: 7.538
Volume 13 Issue V May 2025- Available at www.ijraset.com

Brain Tumor Segmentation Using U-Net3+

Ch. Meghana
Department of Computer Science and Engineering-Emerging Technologies

Abstract: Themeasurementoftumourextentisadifficulttaskinbraintumourtreatmentplanning and quantitative evaluation. Non-invasive magnetic resonance imaging (MRI) has evolved as a first-line diagnostic method for brain malignancies that does not require ionising radiation. The manualsegmentationofbraintumour extent from3DMRI volumes isatime- consuming jobthatheavilyreliesontheoperator'sknowledge.Inthiscontext,adependablefullyautomatic segmentation approach for brain tumour segmentation is required for accurate tumour extent determination. Inthisworkweoffer a fullyautomatic method for braintumour segmentation, whichis basedonU-Net-baseddeepconvolutionalneuralnetworks.Ourtechnique wastested using the Multimodal Brain Tumor Image Segmentation (BRATS 2018) datasets, which included 220 cases of high-grade brain tumour and 54 cases of low-grade tumour. Cross- validation has demonstrated that our method efficiently obtains promising segmentation.
Keywords: Brain tumor segmentation, deep neural networks, U-net, fully convolutional network,BraTS'2018 challenge.

I. INTRODUCTION

A. *Introduction to Primary malignant brain tumors*

Primarymalignantbraintumorsarehighlydevastatingformsofcancer,notonly due to their grim prognosis but also because of the detrimental impact they have on cognitivefunctionandoverallqualityoflife.Themostcommontypesofprimarybrain tumors in adults are primary central nervous system lymphomas and gliomas, with gliomasaccountingfornearly80% ofmalignantcases. Theterm"glioma"encompasses various subtypes of primary brain tumors, ranging from slower growing "low-grade" tumors to highly infiltrative malignant tumors with significant heterogeneity. Despite notableadvancementsinimagingtechniques, radiotherapy,chemotherapy,andsurgical procedures, certain types of malignant brain tumors, such as high-grade glioblastoma andmetastases,arestillconsidereduntreatable,withacumulativerelativesurvivalrate ofonly8%at2.5yearsand2%at10years.Additionally,theprognosisforpatientswith low-gradegliomas(LGG)varies,withanoverall10-yearsurvivalrateofapproximately 57%.

B. *Types of Primary BrainTumors*

Primarybraintumorscanbecategorizedintotwo maintypes:

1) Primarycentralnervoussystemlymphomas
2) Gliomas.

Gliomas are the predominant type among primary brain tumors. Gliomas display considerable diversity, encompassing slow-growing low-grade tumors as well as highly infiltrative malignant tumors**.** Prior research has shown that magnetic resonance imaging (MRI) characteristics of newly identified brain tumors can provide valuable insights into their likely diagnosis and guide treatment strategies. Consequently, multimodal MRI protocols are commonly employed to evaluate brain tumor cellularity, vascularity, and blood-brain barrier (BBB) integrity.

a) PrognosisandSurvivalRates:

Despite recent advancements in semi-automatic and fully automatic algorithms for brain tumor segmentation, there are still several ongoing challenges in this field. These challenges primarily stem from the high variation of brain tumors in terms of size, shape, regularity,location,andtheirheterogeneousappearance,includingfactorssuchascontrast uptake, image uniformity, and texture. Addressing these challenges is crucial to develop robustandaccurate segmentationmethods forbraintumors. Otherpotentialissuesthatmay complicatethebraintumorsegmentationincludeLow-GradeGliomas(LGG)andHigh- Grade Gliomas (HGG) and Challenges in Tumor Sub-region Identification

b) RoleofMRIinBrain TumorDiagnosis

Typical clinical MRI images are often acquired with higher in-plane resolutionbut lower intersliceresolutiontostrikeabalancebetweencoveringtheentiretumor volume withgoodcross-sectionalviewsandlimitedscanningtime.

However,thiscanleadto inadequate signal-to-noise ratio and asymmetrical partial volume effects, which can impact the accuracyofsegmentation. Gaussian hiddenMarkovrandomfield was found to outperform other clustering algorithms for glioblastoma segmentation, but even the best- performing algorithm in that study achieved only 77% accuracy.

c) ImportanceofImageSegmentationinBrain TumorStudies

Imagesegmentationinbraintumorstudies,particularlywithMRIscans,isvitalforprecisediagnosisandtreatmentplanning.Itentailsaccuratel youtliningtumorboundariesagainsthealthy tissues, facilitating an exact classification. This classification is crucial for tailoring appropriate treatment strategies, as differenttumor types and grades may require distinct approaches.

II. RELATED WORK

1) Schwartzbaum, J.A., Fisher, J.L., Aldape, K.D., Wrensch, M.: Epidemiology and molecular pathology of glioma. Nat. Clin. Pract. Neurol. 2, 494–503 (2006) proposed Gliomas account for almost 80% of primary malignant brain tumors, and they result in more years of life lost than do anyother tumors. Glioblastoma, the most common type of glioma, is associated with very poor survival, so glioma epidemiology has focused on identifying factors that can be modified to prevent this disease. Only two relatively rare factors have so far beenconclusivelyshownto affect glioma risk--exposure to highdoses ofionizingradiation,andinheritedmutationsofhighlypenetrantgenesassociatedwithrare syndromes.
2) Smoll,N.R.,Schaller,K.,Gautschi,O.P.:Long-termsurvivalofpatientswithglioblastoma multiforme(GBM). J.Clin. Neurosci. 20,670–675(2013)proposedLong-termsurvivalis anoftenused, yetpoorlydefined,conceptinthestudyofglioblastomamultiforme(GBM). Thisstudysuggestsamethodto defineatime-pointfor long-termsurvivalinpatientswith GBM. Data for this study were obtained from the Surveillance, Epidemiology and End- Results database, which was limited to the most recent data using the period approach. Relative survival measures were used and modelled using piecewise constant hazards to describe the survival profile of long-term survivors of GBM. For patients with GBM, the firstquarterof thesecondyear(5thquarter)post-diagnosis is consideredtobe thepeak incidenceof mortalitywithanexcess hazard ratio of7.58 (95% confidence interval=6.54, 8.78) and the risk of death due to GBM decreases to half of its rate at 2.5 years post- diagnosis.
3) Yamahara, T., Numa, Y., Oishi, T., Kawaguchi, T., Seno, T., Asai, A., Kawamoto, K.: Morphological and flow cytometric analysis of cell infiltration in glioblastoma: a comparison of autopsy brain and neuroimaging. Brain Tumor Pathol. 27, 81–872010 proposedEven when we successfully perform a total extirpation of glioblastoma macroscopically,weoftenencountertumorrecurrence.Weexaminedsevenautopsybrains, focusing on tumor cell infiltration in the peripheral zone of a tumor, and compared our findings with theMRimages. Therehassofarbeennoreportr egardingmappingof tumor cell infiltration and DNA histogram by flow cytometry, comparing the neuroimaging findingswith theautopsybrainfindings. Theautopsybrainwascutin10-mm-thickslices, in parallel with the OM line. Tissue samples were obtained from several parts in the peripheralzone(theouterareaadjacenttothetumoredgeasdefined bypostcontrast MRI) and then were examined byH&E, GFAP, and VEGFstaining.

III. DESIGN AND METHODOLOGY

we aim to perform brain tumor image segmentation using a combination of basic image segmentation and extraction algorithms, employing theU-Net 3+architecture.This approach relies on image analysis techniques to accurately delineate tumor regions.

Proper classification plays a crucial role in achieving accurate segmentation. By leveraging our proposed method, we can ensure appropriate classification, leading to precise tumor segmentation.Toillustratetheprocessvisually **Fig**,ablockdiagramofourproposedmethod is provided below.

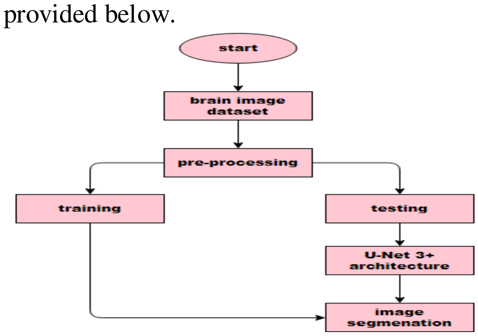

Fig:Blockdiagramofproposedmethod

1) Input Preprocessing:

Acquire medical imaging data, such as MRI scans, containing brain tumor images. Perform preprocessingsteps,includingimagenormalization,intensityadjustment,andnoisereduction, to enhance the quality and consistency of the input data.

2) U-Net3+ArchitectureOverview:

The U-Net 3+ architecture consists of an encoder-decoder structure with dense skip connections,allowing forimproved informationflowandfeaturereuse.Thearchitectureaimstocapturebothlocalandglobalcontextinformation,facilitatingaccuratesegmentationofbrain tumors.

3) EncoderModule:

Theencodermodule comprises a series ofconvolutional layers followed bypooling layersto graduallydownsampletheinputimage.Eachconvolutionallayerappliesfilterstoextracthigh- level features from the input, capturing important patterns and structures. The pooling layers reduce spatial dimensions, enabling the network to capture more abstract information while preserving important features.

4) DecoderModule:

The decoder module reconstructs the spatial information by upsampling the feature maps obtained fromthe encoder. Eachupsampling step isaccompanied byskip connections, which concatenatefeaturemapsfromthecorresponding encoder levels.Theskipconnectionsenable the U-Net 3+ architecture to combine high-resolution details from earlier layers with the contextual information captured at deeper levels.

Contrast Limited AHE (CLAHE) - is a variant of adaptive histogram equalization that addresses theproblemofnoiseamplification. It limits theamplificationofcontrast tomitigate this issue. In CLAHE, the degree of contrast amplification near a specific pixel value is determined by the slopeofthetransformationfunction.Imageenhancementtechniquesaimtoimprovethevisual quality of an image as perceived by humans.

Normalize: Image normalization is a common technique in image processing that adjuststherangeofpixelintensityvalues. Itsprimarypurposeistoconvertaninput imageintoarangeof pixel values that are more standard or typical, hence the term "normalization.

BiomedicalImageSegmentation

- Re-designedSkipPathways
- DeepSupervision
- ExperimentalResults

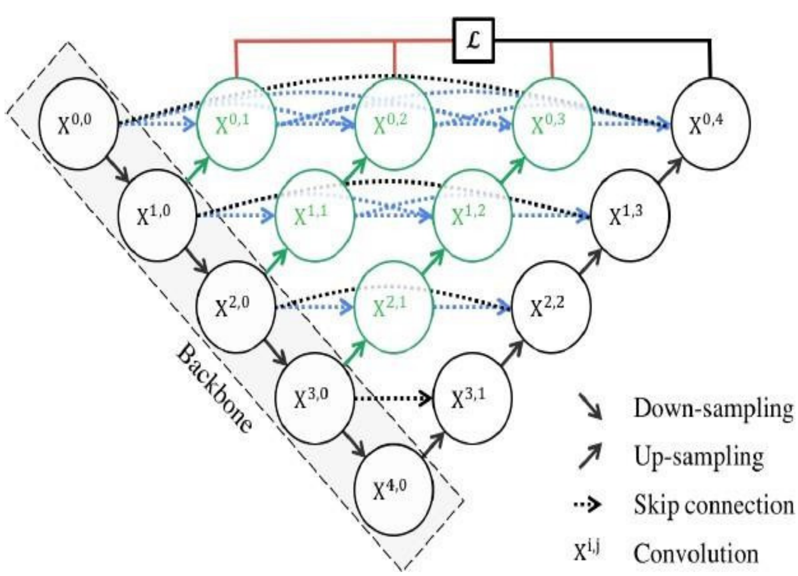

Fig:Working PrincipleofUnet+Architecture

The U-Net architecture is named after itsdistinct U-shaped structure,which isevident froma brief observation of the above diagram**.**The architecture is characterized by its fully convolutional nature, meaning it primarily consists of convolutional layers and lacks other types of layers such as dense or flatten layers.

The architecture is divided into two main parts: the contracting path and the expanding path. The contracting path captures the context and reduces the spatial dimensions of the input through a series of convolutional and pooling layers. This path is often referred to as the encoder as it encodes the input into a lower-dimensional representation.

IV. UNET3+ARCHITECTURE

TheU-Net3+architectureisanextensionoftheoriginalU-Netarchitecturespecifically designed for brain tumor segmentation. It aims to improve the performance of tumor segmentation by incorporating additional features and skip connections.

TheU-Net3+architectureconsistsofthreemaincomponents:thecontractingpath,thebridge, and the expansive path. These components work together to capture both local and global context information and enable precise tumor segmentation.

1) ContractingPath:

The contracting path in U-Net 3+ is similar to the originalU-Net architecture. It consists of several encoder blocks, each consisting of two convolutional layers followed by batch normalization and ReLU activation. The encoder blocks progressivelydownsample the input image,capturinghigh-levelfeaturesandreducingthespatialdimensions.Skipconnectionsare created at each level by concatenating the output of each encoder block to the corresponding decoder block.

2) Bridge:

The bridge in U-Net 3+ is a modification that enhances the original architecture. It introduces a "3+" block, which consists ofthree convolutional layers. The 3+ block is placed afterthe finalencoderblockand helps capturemoredetailed informationand improve feature representation.

3) ExpansivePath:

The expansive path is responsible for upsampling the feature maps and reconstructing the segmentedimage. Itconsistsofdecoderblocksthatareconnectedtotheircorrespondingencoder blocks through skip connections. Each decoder block performs upsampling using transpose convolutions (also known as deconvolutions) to increase the spatial dimensions

UnderstandingtheWorkingofU-Net3+ArchitectureforBrain TumorSegmentation

The U-Net 3+ architecture is specifically designed for brain tumor segmentation, aiming to improve the accuracyand performance ofthe segmentationprocess.

It incorporates skip connections and additional features to capturebothlocaland globalcontext information. The braintumor segmentationprocess using the U-Net 3+ architecture canbe summarized in the following steps:

4) Preprocessing:

Before applying theU-Net 3+model,thebraintumor imagesarepreprocessedto enhance their qualityand standardize their characteristics. This may involve steps such as resizing the images, normalizing pixel intensities, and applying contrast enhancement techniques.

5) Encoding:

Theencodingphasebeginswiththeinputbraintumorimage.TheimageispassedthroughaseriesofencoderblocksinthecontractingpathoftheU-Net3+architecture.Eachencoder block consists of two convolutional layers followed by batch normalization and ReLU activation.Theseblockscaptureandextracthigh-levelfeaturesfromtheinputimagewhile progressively reducing the spatial dimensions.

6) Skip Connections:

At each level in the contracting path, skip connections are created by concatenating the outputofthe corresponding encoder block withthe input ofthe decoderblock atthe same level. These skip connections enable the model to retain and utilize detailed information from earlier layers during the decoding process.

International Journal for Research in Applied Science & Engineering Technology (IJRASET)
ISSN: 2321-9653; IC Value: 45.98; SJ Impact Factor: 7.538
Volume 13 Issue V May 2025- Available at www.ijraset.com

7) Bridge:
After the final encoder block, the U-Net 3+ architecture introduces a "3+" block in the bridge. This block consists of three convolutional layers and helps capture more detailed information and enhance the feature representation.

8) Decoding:
Thedecodingphasebeginswiththebridgeoutputandproceedsthroughaseriesofdecoder blocks in the expansive path of the U-Net 3+ architecture. Each decoder block performs upsampling using transpose convolutions to increase the spatial dimensions.The skip connections from the contracting path are used to concatenate the features from the corresponding encoder blocks, allowing the model to access both high-level and detailed information during the upsampling process.

9) OutputLayer:
The output layer of the U-Net 3+ architecture consists of a convolutional layer followed bya softmaxactivation function. This finallayer generates the segmented tumor mask,highlightingthetumorregionsintheinputimage.Thepredictedmaskcanbefurtherpost-processed to refine the segmentation results if necessary.
UnderstandingtheWorkingStructureofU-Net3+Architecture

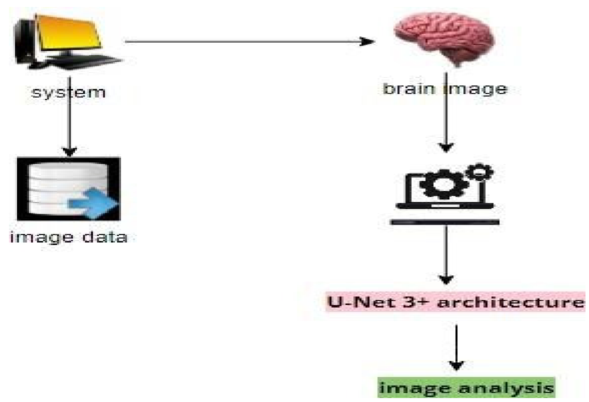

V. DATASET AND DATA PREPARATION

A. Data Set:
The BraTS' 2018 contest offers a large dataset for training. It includes 210 MRI scans for High-GradeGlioma(HGG)and75MRIscansforLow-GradeGlioma(LGG).EachMRIscan hasdimensionsof240x240x155,andtheycontainFLAIR,T1,T1-enhanced,andT2volumes. The dataset has undergone co-registration, resampling to 1 mm³, and skull- stripping. An exampleofthedataanditscorrespondinggroundtruthisdepictedin**Fig:5.1.1(a)**.Thegoalof thedatasetistosegmentvarioustypesofbraintumors,suchasnecrosis,edema,non-enhancing, and enhancing tumors.

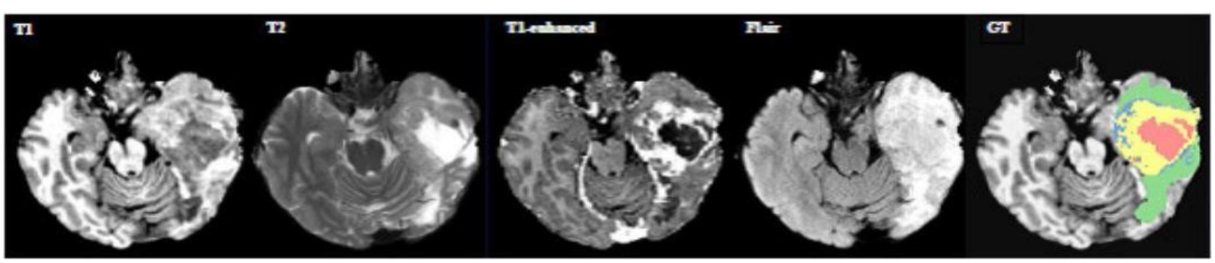

Fig: 5.1.1(a). Sample MRI images and ground truth labels, from left to right, T1, T2, T1- enhanced, and the label images; Green: edema, yellow: enhancing tumor, red: necrosis and non-enhancing.

ThecommonMRIsequencesusedasinputforbraintumorsegmentationwithU-Net architecture are:

1) T1-weighted (T1) image: This MRI sequence highlights the contrast between different brain tissues based on the relaxation time of protons. T1-weighted images are useful for visualizing anatomical structures and are often used as a baseline for comparing other MRI sequences.

International Journal for Research in Applied Science & Engineering Technology (IJRASET)
ISSN: 2321-9653; IC Value: 45.98; SJ Impact Factor: 7.538
Volume 13 Issue V May 2025- Available at www.ijraset.com

2) T2-weighted (T2) image: T2-weighted MRI sequences are sensitive to the differences in water content and are particularly useful for detecting edema, inflammation, and fluid-filled structuresinthebrain. Tumorsoftenexhibitdifferentsignalintensitieso nT2-weightedimages compared to surrounding healthy tissue.
3) T1-contrast-enhanced (T1-Enhanced) image: In this MRI sequence, a contrast agent (such as gadolinium) is administered intravenously to enhance the visualization of vascular structuresandareaswithdisruptedblood-brainbarrier, suchastumortissue. Tumorstypically showenhanced uptakeofthecontrastagent,leadingtobetterdelineationoftumorboundaries.
4) FLAIR:FLAIRimagessuppressthesignalfromCSF,resultinginahighcontrastbetween CSF-filled spaces and surrounding tissues. This property makes FLAIR images valuable for detecting abnormalities, including brain tumors, and for visualizing tumor margins and peritumoral edema.
5) Ground Truth (GT) image orMask: This image serves as the reference or gold standard for brain tumor segmentation. It is a binarymask where eachpixel is labelled as either tumor or background (non-tumor). Ground truth masks are typically manually annotated by experts or derived from histological analysis.

B. UNET 3+ Implementation: WorkingofUnet3+Architecture:

TheU-Net 3+ architectureis distinguished byits encoder and decodercomponents.In this setup, the decoder initiates its operations following the downsampling ofthe feature map to 2x2x2. While maintaining modularity, the decoder's primary task is to refine the encoder's featuremaptoenhancespatialdimensions.Eachdecoderblockcomprisesthreesmallerblocks.

The encoder consists of five interconnected blocks, each with pooling operations and convolutionalblockswithspecific filters. Thefifthblock actsasabottleneck layer.Similarly, the decoder consists of five blocks, with each layer concatenated with the preceding and encodinglayers.BatchnormalizationandReLUactivationareappliedtoeachlayerexceptthe last. Full-scale skip connections facilitate connectivity between the encoder and decoder, as well as within the decoder sub-networks.

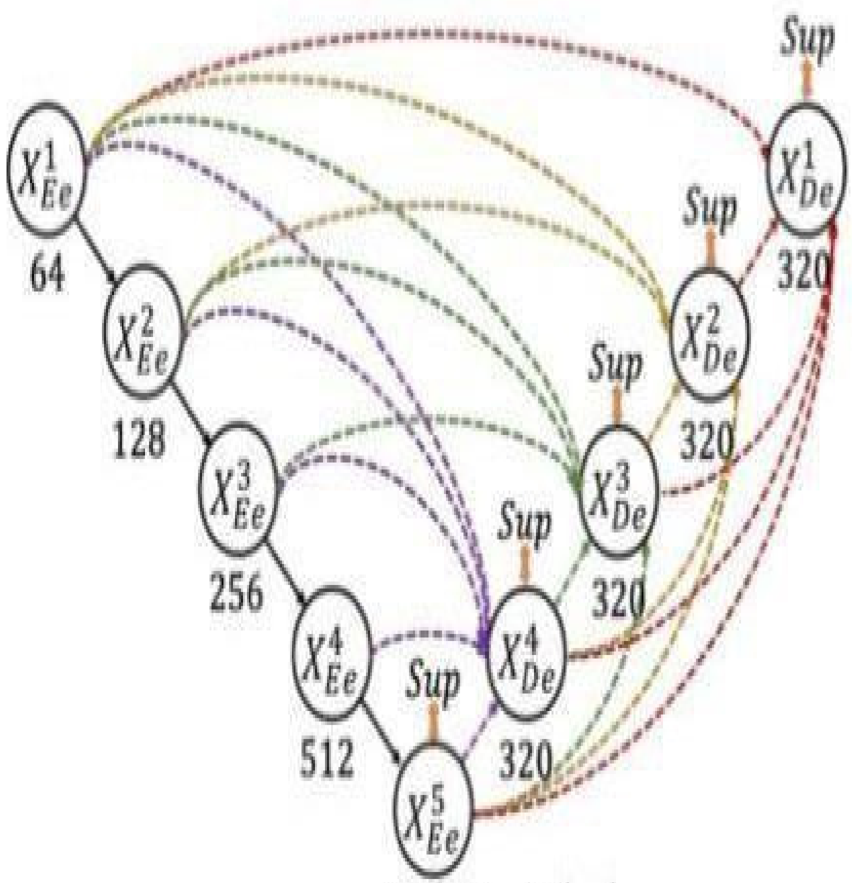

U-Net3+ Architecture

VI. ANALYSIS AND RESULTS

A. *TrainingDataintoU-Net3+Model:*

```
Model: "UNet_3Plus"
__________________________________________________________________________________________________
Layer (type)                   Output Shape         Param #     Connected to
==================================================================================================
input_layer (InputLayer)       [(None, 128, 128, 3) 0
__________________________________________________________________________________________________
conv2d (Conv2D)                (None, 128, 128, 64) 1792        input_layer[0][0]
__________________________________________________________________________________________________
batch_normalization (BatchNorma (None, 128, 128, 64) 256        conv2d[0][0]
__________________________________________________________________________________________________
tf.nn.relu (TFOpLambda)        (None, 128, 128, 64) 0           batch_normalization[0][0]
__________________________________________________________________________________________________
conv2d_1 (Conv2D)              (None, 128, 128, 64) 36928       tf.nn.relu[0][0]
__________________________________________________________________________________________________
batch_normalization_1 (BatchNor (None, 128, 128, 64) 256        conv2d_1[0][0]
__________________________________________________________________________________________________
tf.nn.relu_1 (TFOpLambda)      (None, 128, 128, 64) 0           batch_normalization_1[0][0]
__________________________________________________________________________________________________
max_pooling2d (MaxPooling2D)   (None, 64, 64, 64)   0           tf.nn.relu_1[0][0]
__________________________________________________________________________________________________
conv2d_2 (Conv2D)              (None, 64, 64, 128)  73856       max_pooling2d[0][0]
__________________________________________________________________________________________________
batch_normalization_2 (BatchNor (None, 64, 64, 128)  512        conv2d_2[0][0]
__________________________________________________________________________________________________
tf.nn.relu_2 (TFOpLambda)      (None, 64, 64, 128)  0           batch_normalization_2[0][0]
...
Total params: 26,984,833
Trainable params: 26,971,777
Non-trainable params: 13,056
```

```
Epoch 1/5
WARNING:tensorflow:From C:\Users\surya\anaconda3\Lib\site-packages\keras\src\utils\tf_utils.py:492: The name tf.ragged.RaggedTe
nsorValue is deprecated. Please use tf.compat.v1.ragged.RaggedTensorValue instead.

WARNING:tensorflow:From C:\Users\surya\anaconda3\Lib\site-packages\keras\src\engine\base_layer_utils.py:384: The name tf.execut
ing_eagerly_outside_functions is deprecated. Please use tf.compat.v1.executing_eagerly_outside_functions instead.

20/20 [==============================] - ETA: 0s - loss: 1.4505 - accuracy: 0.9157 - iou: 0.0724 - dice_coef: 0.1307
Epoch 1: val_loss improved from inf to 3.00059, saving model to model-brain-mri.h5
20/20 [==============================] - 1443s 73s/step - loss: 1.4505 - accuracy: 0.9157 - iou: 0.0724 - dice_coef: 0.1307 - v
al_loss: 3.0006 - val_accuracy: 0.9920 - val_iou: 3.9444e-05 - val_dice_coef: 7.8888e-05 - lr: 0.0010
Epoch 2/5
20/20 [==============================] - ETA: 0s - loss: 1.2039 - accuracy: 0.9887 - iou: 0.2235 - dice_coef: 0.3582
Epoch 2: val_loss improved from 3.00059 to 1.28941, saving model to model-brain-mri.h5
20/20 [==============================] - 4501s 229s/step - loss: 1.2039 - accuracy: 0.9887 - iou: 0.2235 - dice_coef: 0.3582 -
val_loss: 1.2894 - val_accuracy: 0.9855 - val_iou: 0.0337 - val_dice_coef: 0.0648 - lr: 0.0010
Epoch 3/5
20/20 [==============================] - ETA: 0s - loss: 1.0166 - accuracy: 0.9891 - iou: 0.2157 - dice_coef: 0.3434
Epoch 3: val_loss improved from 1.28941 to 0.95119, saving model to model-brain-mri.h5
20/20 [==============================] - 1992s 97s/step - loss: 1.0166 - accuracy: 0.9891 - iou: 0.2157 - dice_coef: 0.3434 - v
al_loss: 0.9512 - val_accuracy: 0.9912 - val_iou: 0.0472 - val_dice_coef: 0.0896 - lr: 0.0010
Epoch 4/5
20/20 [==============================] - ETA: 0s - loss: 0.8415 - accuracy: 0.9916 - iou: 0.1766 - dice_coef: 0.2869
Epoch 4: val_loss improved from 0.95119 to 0.79544, saving model to model-brain-mri.h5
20/20 [==============================] - 1192s 59s/step - loss: 0.8415 - accuracy: 0.9916 - iou: 0.1766 - dice_coef: 0.2869 - v
al_loss: 0.7954 - val_accuracy: 0.9902 - val_iou: 0.0280 - val_dice_coef: 0.0537 - lr: 0.0010
Epoch 5/5
20/20 [==============================] - ETA: 0s - loss: 0.6994 - accuracy: 0.9908 - iou: 0.2637 - dice_coef: 0.4073
Epoch 5: val_loss improved from 0.79544 to 0.68281, saving model to model-brain-mri.h5
20/20 [==============================] - 1046s 53s/step - loss: 0.6994 - accuracy: 0.9908 - iou: 0.2637 - dice_coef: 0.4073 - v
al_loss: 0.6828 - val_accuracy: 0.9918 - val_iou: 0.0402 - val_dice_coef: 0.0765 - lr: 0.0010
```

AccuracyoftheModel

After training the model with the data, validation is conducted to prevent data redundancies. Subsequently,upon applying the UNET 3+ modelto the trained dataset, tumors areaccurately identified and segmented.

International Journal for Research in Applied Science & Engineering Technology (IJRASET)
ISSN: 2321-9653; IC Value: 45.98; SJ Impact Factor: 7.538
Volume 13 Issue V May 2025- Available at www.ijraset.com

LossFunctionGraph:

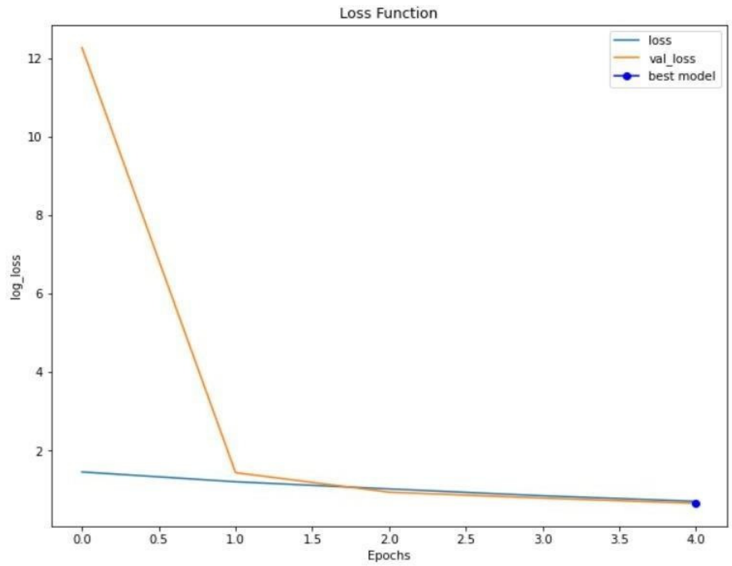

LossFunction Graph

Alossfunctiongraphwithlogloss(cross-entropyloss)onthex-axisandepochsonthey-axisvisualizes how the loss changes over the course of training. Here's how to interpret it:

- X-axis (Log Loss): Log loss, also known as cross-entropy loss, measures the difference between the predictedprobabilitydistributionandthetruedistributionofthedata.Itquantifieshowwellthemodel's predictions match the actual labels. The lower the log loss, the better the model's performance.
- Y-axis (Epochs): Epochs represent the number ofcomplete passes throughthetraining dataset during thetrainingprocess. Eachepochcorrespondstoonecycleoftraining, where themodellearns fromthe data and updates its parameters to minimize the loss function.
- Graph: The graph plots log loss (cross-entropy loss) onthe x-axis and epochs on the y-axis. As training progresses (moving from left to right along the x-axis), the loss ideallydecreasesoversuccessiveepochs (movingfromtoptobottomalongthey-axis).Thisindicatesthatthemodelislearningandimprovingits performanceover time.

FinalAccuracy:

20/20[==============================]-ETA:0s-loss:1.4505-accuracy:

0.9157-iou:0.0724-dice_coef:0.1307

Epoch1:val_lossimprovedfrominf to3.00059, savingmodeltomodel-brain-mri.h520/20
[==============================]-1443s73s/step-loss:1.4505-
accuracy:0.9157-iou:0.0724-dice_coef:0.1307-val_loss:3.0006-val_accuracy:0.9920 - val_iou: 3.9444e-05 - val_dice_coef: 7.8888e-05 - lr: 0.0010
Epoch2/5

11/20[===============>..............]-ETA:26:19-loss:1.2450-accuracy:0.9887-

iou:0.2274-dice_coef:0.3609

InputData:

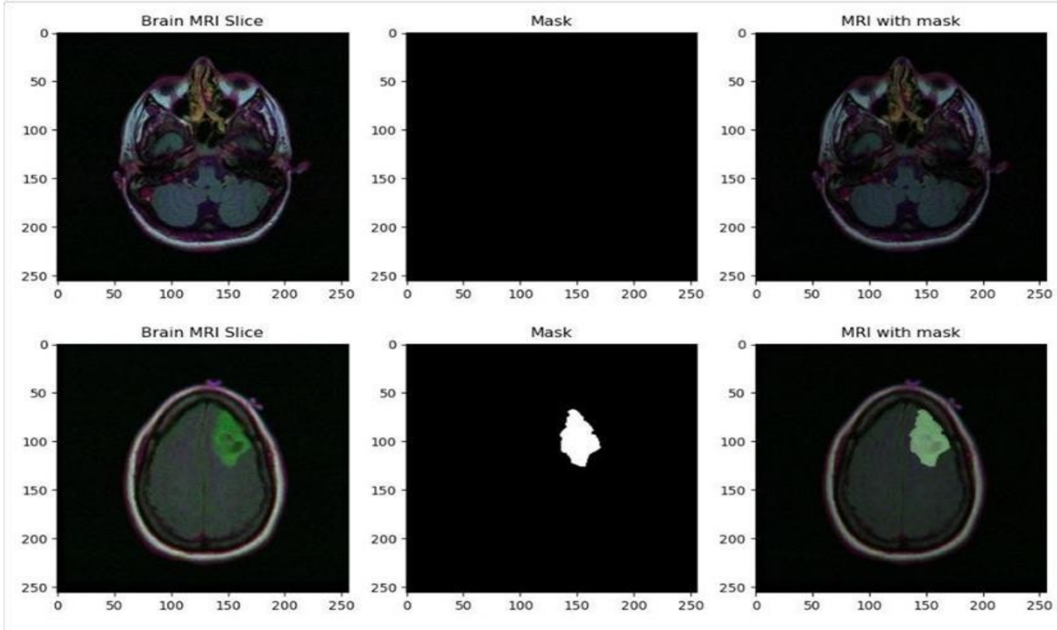

InputMRIScanImages

VII. IMPLEMENTATION RESULTS

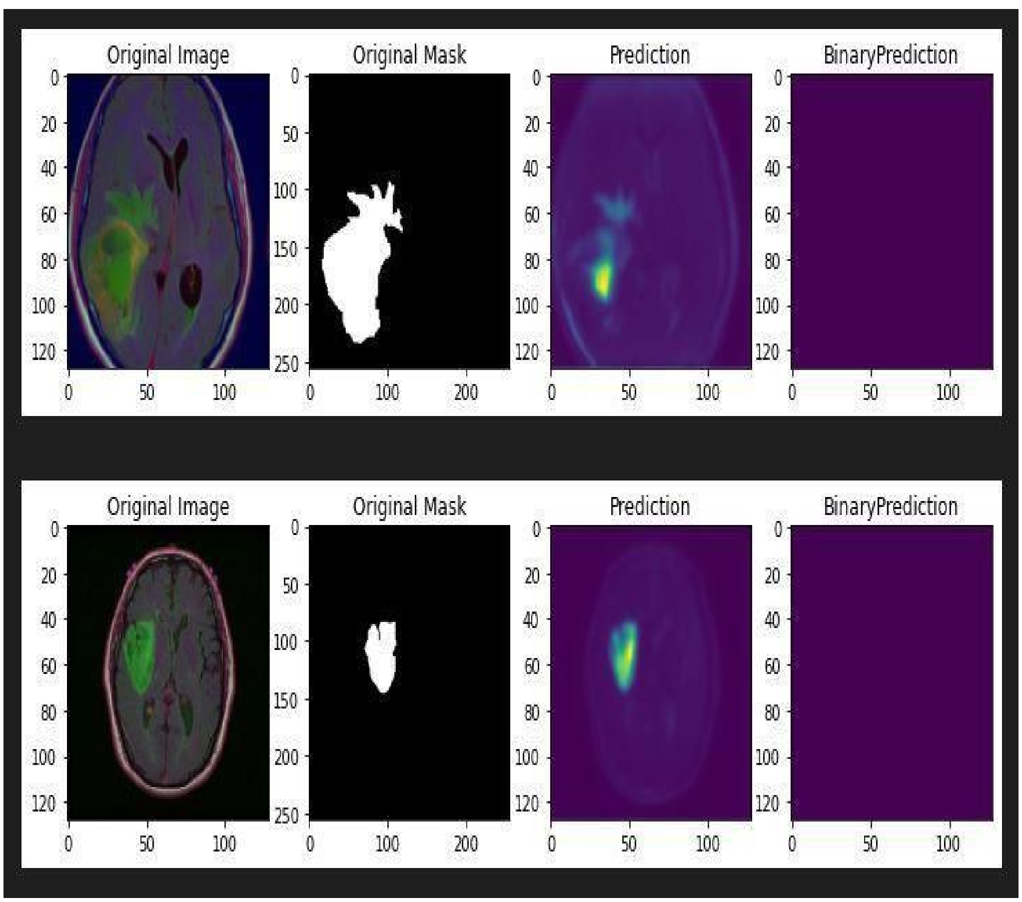

(a)

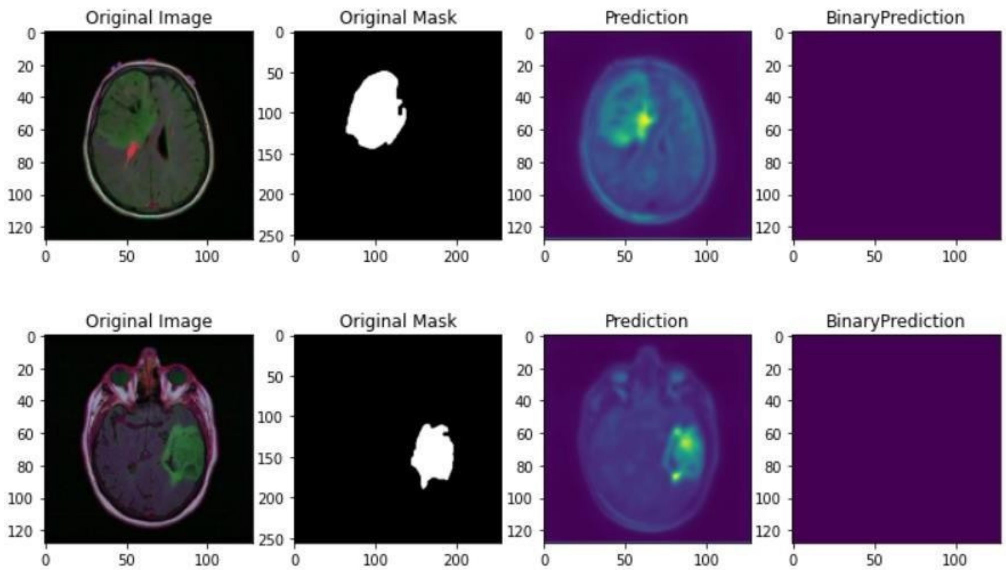

(b)

VIII. CONCLUSION

Inconclusion,thisprojectfocusedonthesegmentationofbraintumorimagesusingtheadvanced U-Net 3+ architecture. We successfully completed the task by employing a dataset specifically curated for brain tumor segmentation. The U-Net 3+ architecture, known for its abilityto capture detailed informationat different scales, was trained using the dataset(BRATS 2018). During the training phase, the modellearned to accuratelyidentifyandsegmenttumorregionsinthebrainimages.Thissegmentationprocessinvolved differentiating the veins from the tumor regions, effectively highlighting the areas of interest.

IX. FUTURE SCOPE

There is scope for further feature enhancement and exploration in the UNet3+ architecture for brain tumorsegmentation. Here are a few potential areas of improvement and feature scope:

1) Firstly, there's potential for refining the model's performance through optimization efforts, such as experimenting with differentactivationfunctionsandlayerconfigurationstoenhance accuracy and efficiency.
2) Additionally, integrating multiple imaging modalities like MRI, CT, or PET scans could improve segmentation results by effectively combining information from different sources.

REFERENCES

[1] Schwartzbaum, J.A., Fisher, J.L., Aldape, K.D., Wrensch, M.: Epidemiologyand molecular pathologyof glioma. Nat. Clin. Pract. Neurol. 2, 494–503 (2006)
[2] Smoll, N.R., Schaller, K., Gautschi, O.P.: Long-term survival of patients with glioblastoma multiforme (GBM). J. Clin. Neurosci. 20, 670–675 (2013)
[3] Ramakrishna, R., Hebb, A., Barber, J., Rostomily, R., Silbergeld, D.: Outcomes in reoperated low-grade gliomas. Neurosurgery 77, 175–184 (2015)
[4] Mazzara,G.P.,Velthuizen,R.P.,Pearlman,J.L.,Greenberg,H.M.,Wagner,H.:Braintumortargetvolume determinationforradiationtreatmentplanningthroughautomatedMRIsegmentation.Int.J.Radiat.Oncol. Biol. Phys. 59, 300–312 (2004)
[5] Yamahara,T.,Numa,Y.,Oishi,T.,Kawaguchi,T.,Seno,T.,Asai,A.,Kawamoto,K.:Morphologicaland flow cytometric analysis of cell infiltration in glioblastoma: a comparison of autopsy brain and neuroimaging. BrainTumor Pathol. 27,81–87(2010)
[6] Bauer, S., Wiest, R., Nolte, L.-P., Reyes, M.: A survey of MRI-based medical image analysis for brain tumorstudies.Phys.Med.Biol.58,R97–R129(2013)AutomaticBrainTumorDetectionandSegmentation 515
[7] Jones,T.L.,Byrnes,T.J.,Yang,G.,Howe,F.A.,Bell,B.A.,Barrick,T.R.:Braintumorclassificationusing the diffusion tensor image segmentation (D-SEG) technique. Neuro. Oncol. 17, 466–476 (2014)
[8] Soltaninejad,M.,Yang,G.,Lambrou,T.,Allinson,N.,Jones,T.L.,Barrick,T.R.,Howe, F. A., Ye, X.: Automated brain tumour detection and segmentation using superpixel- based extremely randomized trees in FLAIR MRI. Int. J. Comput. Assist. Radiol. Surg. 12(2), 183– 203 (2016)
[9] Szilágyi, L.,Lefkovits,L.,Benyó,B.:Automatic braintumorsegmentationin multispectralMRI volumes using a fuzzy c-means cascade algorithm. In: 2015 12th International Conference on Fuzzy Systems and Knowledge Discovery (FSKD), pp. 285– 291 (2015)
[10] Mei, P.A., de Carvalho Carneiro, C., Fraser, S.J., Min, L.L., Reis, F.: Analysis of neoplastic lesions in magnetic resonance imaging using self-organizing maps. J. Neurol. Sci. 359, 78– 83 (2015)

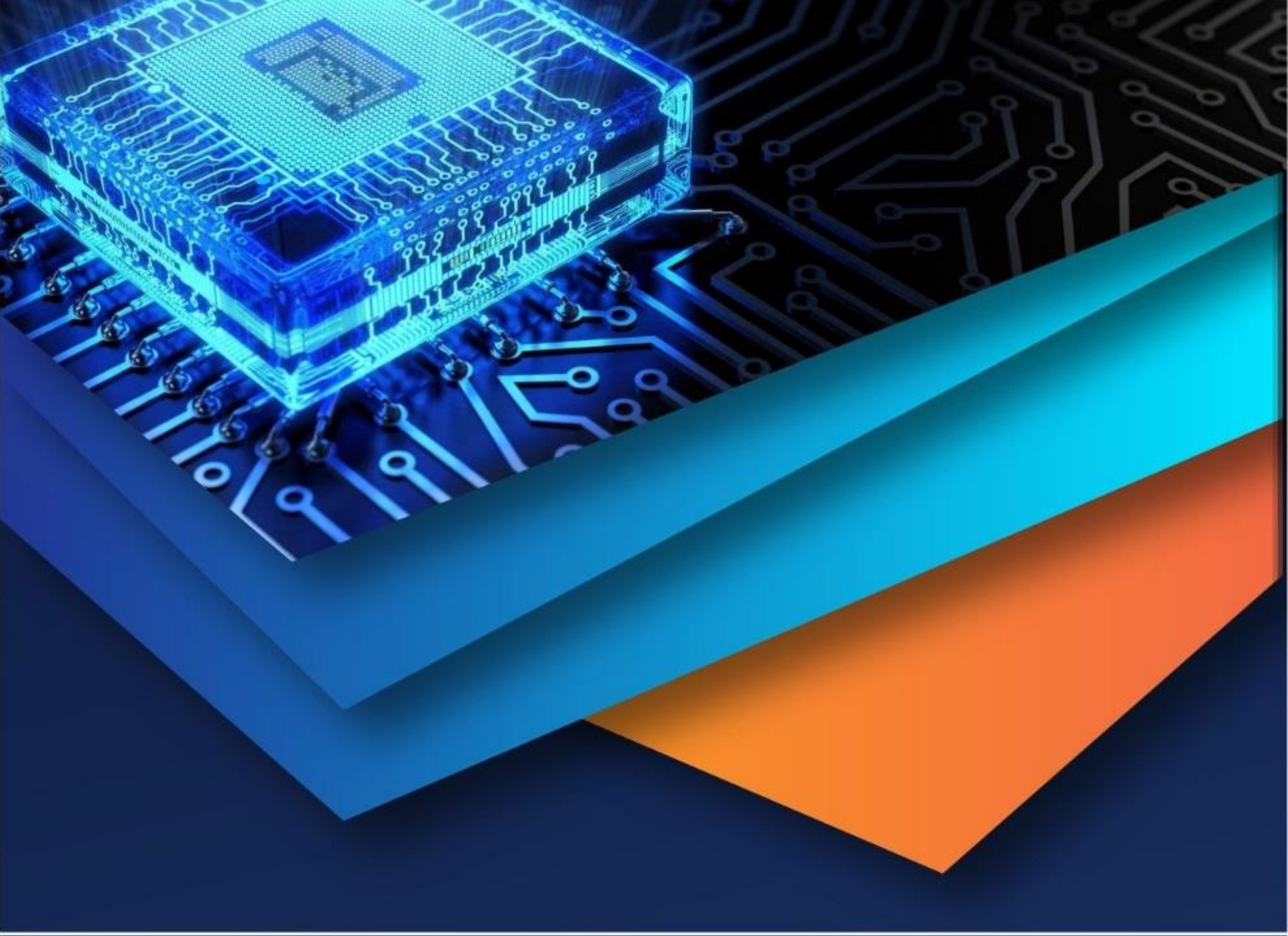

10.22214/IJRASET

INDEX COPERNICUS
45.98

IMPACT FACTOR:
7.129

TOGETHER WE REACH THE GOAL
IMPACT FACTOR:
7.429

INTERNATIONAL JOURNAL FOR RESEARCH

IN APPLIED SCIENCE & ENGINEERING TECHNOLOGY